A Relationship Between Brittle Fracture Strength and the Nucleation Point in a Fractured Surface

By Akio TAKIMOTO*, Takao KAWAMOTO**, Yoshio KOUHASHI***

(Received July 15, 1981)

Abstract

Fracture strength referred particularly to the eccentric initiation in a fractured surface has been investigated in employing a brittle plastic sheet and FCD-50 cast iron. Micro-faults like a craze and inclusion particles play a role of a nucleus in the homogeneous plastics. Micro-bubbles introduced purposely into the plastics control the fracture initiation sites in the non-homogeneous material. Nodular graphite particles in FCD-50 are the inevitable fracture nucleation sources. A ferrous sphere of 0.7 or 2.0mm dia. or a glass sphere of 0.5 or 2.0mm dia. artificially introduced into the plastics also controls a fracture initiation site. All such nucleation points in fractured surfaces have been analyzed by a plane eccentricity and by a relative distance to the free boundary proposed herewith. Fracture strength is shown to be functions of these. Discussion is made on these including the basic and the current knowledge on the stress concentration factor on an off site second phase and the stress distributions around a spherical solid in the continuum and the interfacial bonding condition between a second spherical phase and the matrix.

1. Introduction

Stress distributions around a spherical cavity[1] or solid[4] in an elastic continuum have been solved by the three dimensional elastic analysis and the stress concentration factors have been obtained experimentally by using the three dimensional photoelastic method[2]. Photoelastic results in the frozen technique have shown that the stress concentration factor of a spherical cavity near the free surface becomes larger, approaching to an infinite value as it comes closer to the free boundary. Those works so far published, however, have included no discussion on the relationships among the interfacial bonding condition between a spherical solid and a matrix, an eccentric locational condition of a spherical second phase in a plane normal to the applied load, brittle fracture strength and so on.

By employing the micro-bubbles purposely introduced in a brittle plastic sheet and the nodular graphite particles in FCD-50 as the spherical cavities and an artificially introduced small sphere of iron or glass in a brittle plastic sheet as a spherical solid, we have studied the effects of the plane eccentricity and the size of a spherical second phase and the interfacial bonding condition between them on brittle fracture. Effect of the eccentricity of a fracture nucleus in a homogeneous plastic sheet has also been investigated.

* Department of Industrial Mechanical Engineering
** Graduate Student, Industrial Mechanical Engineering
*** Hitachi Seisakusho Co., LTD

2. Experimental Procedure

A brittle plastic sheet used as an elastic continuum, was made from the mixture of the thermosetting unsaturated polyester resin, Rigolac 1557C, the hardner (M. E. K. P.) and the promoter, Cobalt-N. The proper mixture was casted in the form of a thin sheet and the necessary heat treatments of homogenizing at 80°C and of slow cooling to the room temperature were performed on this. Specimens of the homogeneous solid, namely A1～A5, were prepared from this sheet. Multiple micro-bubbles were introduced into the material by stirring the liquid mixture, which was casted and heat-treated as mentioned above. Specimens containing micro-bubbles, so-called the nonhomogeneous ones, namely B1～B5 were made from this solid. The sheet material of having a small ferrous or glass sphere at the expected location in a plane normal to the applied load was prepared by casting the mixture twice intermittently and was heat-treated as the above. The C-Type specimens were cut out from this. The 0.7 and 2.0mm dia. spheres of iron and the 0.5 and 2.0mm ones of glass were used in these tests as a matter of experimental convenience. Surfaces of all plastic specimens were carefully polished with waterproof papers of silicon carbide and buff cloth. A practical material, FCD-50 of a nodular cast iron was also employed as an application test. A small specimen was machined from the castings and heated to 800°C in the argon-atmospheric furnace for a few minutes and successively quenched into the warm water of 50°C to obtain the very brittle matrix of martensite. Fig. 1 shows dimensions of all these specimens.

Tensile fracture tests were performed on these with the developed Adams-type tensile

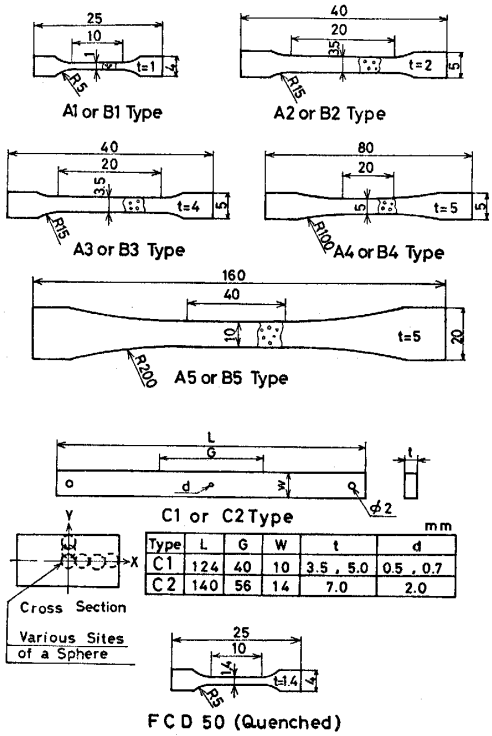

Fig. 1 Dimensions of specimens.

machine of the maximum load of 500kgf at the temperature of 7±3°C for the plastic specimens and at 5±2°C for FCD-50 specimens to attain more brittle condition.
Micro-bubble distributions were examined for all nonhomogeneous specimens tested under the optical photomicrographs. The nucleation, the point at which fracture initiated in a fractured surface, was studied by the use of optical photomicrographs for homogeneous and nonhomogeneous plastic specimens and for FCD-50 specimens by the SEM photographs. The various kinds of nuclei in the homogeneous specimens, the plane eccentricity (E_{C3}) of a nucleus, the surface area of a sphere appeared above the fracture surface and so on were investigated. The bonding condition between a sphere and the plastic matrix was also examined in the preliminary tensile test and was used as a clue to understand the fracture behavior.

3. Experimental Results

To study the relationship between fracture strength and a nucleation point in a fractured surface, the way of defining the eccentricity of the point is required. We first define the X directional eccentricity $E_{C1}=e_X/W$, where e_X is the eccentricity in the X direction in a fractured surface and W is the half width of a specimen and the Y directional eccentricity $E_{C2}=e_Y/t$ in the same way except that W is replaced by t, the half thickness of a specimen. Then, the plane eccentricity, E_{c3} is defined by Eq. (1).

$$E_{C3}=\sqrt{\{(E_{c1})^2+(E_{c2})^2\}/2}=\sqrt{\{(e_x/W)^2+(e_y/t)^2\}/2} \quad \cdots(1)$$

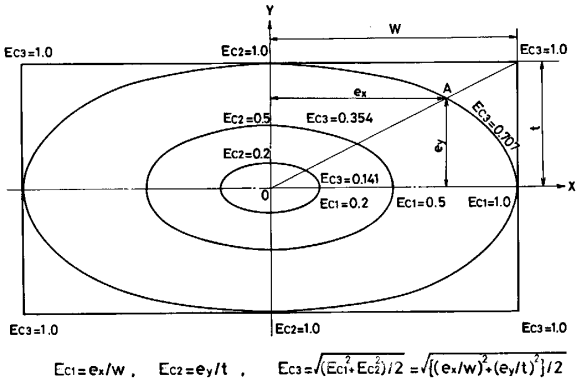

Fig. 2 A schematic presentation of the contour of an equal plane eccentricity in a fractured surface.

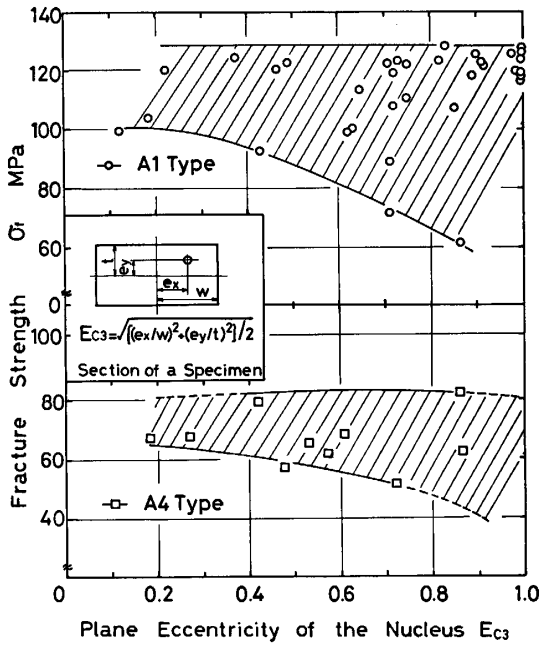

Fig. 3 Variation of fracture strength is shown with respect to the eccentricity of the nucleus in a fractured surface for the homogeneous specimens (A-Types).

Since this equation indicates an ellipse having the transverse axis of E_{C1} and the vertical axis of E_{C2}, an ellipse will show an equal plane eccentricity locus in a fractured surface.

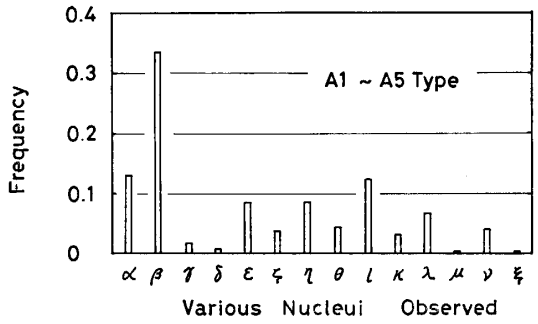

Fig. 4 Variation in frequency of finding a similar nucleus is expressed in the histogram. Various nuclei are arranged in the order of higher strength. The highest one is at the left end and the lowest at the right.

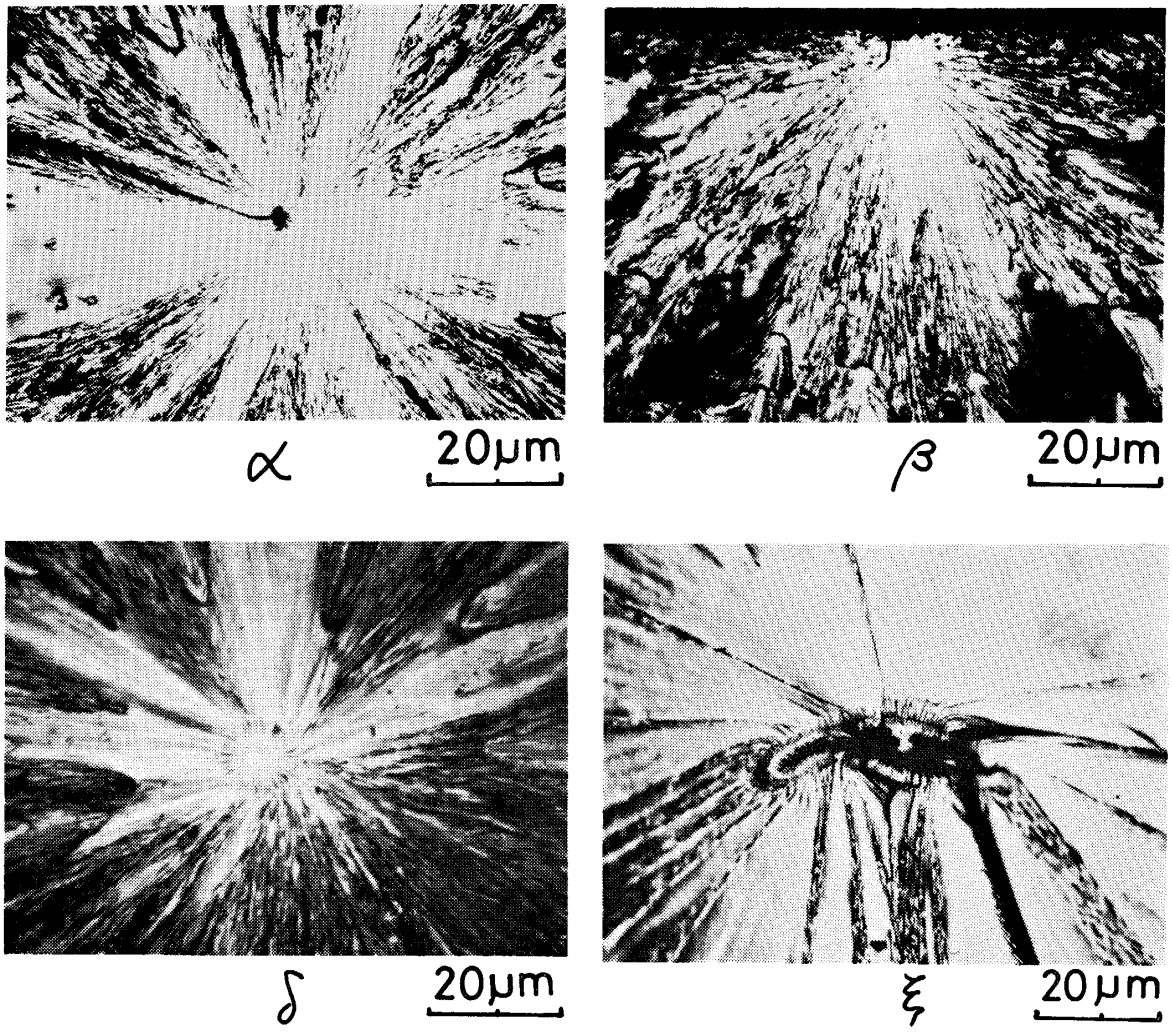

Photo 1 Examples of four different nuclei observed in U. P. as defined α, β, δ and ξ, respectively.

This is shown schematically in Fig. 2.

In a homogeneous specimen fracture nucleates at a material's fault like a craze or at an inclusion, where a nucleus is usually found in a fractured surface. The lower limit of fracture strength decreases as the plane eccentricity of the nucleus increases as shown in Fig. 3. Results on A1 specimens (the top diagram) and on A4 specimens (the bottom) are reported. The former indicates higher strength than the latter due to the size effect and the higher strength specimens have naturally larger scattering in strength. Various kinds of nuclei have been observed in these specimens and the frequency of finding the similar one is examined and is expressed in a histogram in Fig. 4. Fourteen different nuclei are classified by their configurations and are put in the order of higher strength starting from the Greek letter, α. The β-type nucleus, initiated at the free boundary, is found most often in all size specimens out of 188 piecies. Four different nuclei of α, β, δ and ξ are exampled in Photo 1.

In specimens containing multiple micro-bubbles, the nonhomogeneous material, the loss in strength due to the increment of the plane eccentricity is shown in Fig. 5. Results on B1 specimens, in the top diagram, show widely scattered strength but the upper and lower bounds will give the correct information. The wide scattering may due to the fact that the variation of the bubble diameter is relatively large compared with the cross section of this type specimen, in addition to the fact that it has higher strength due to its small volume. The bottom one in Fig. 5 shows the results on B5 specimens. The

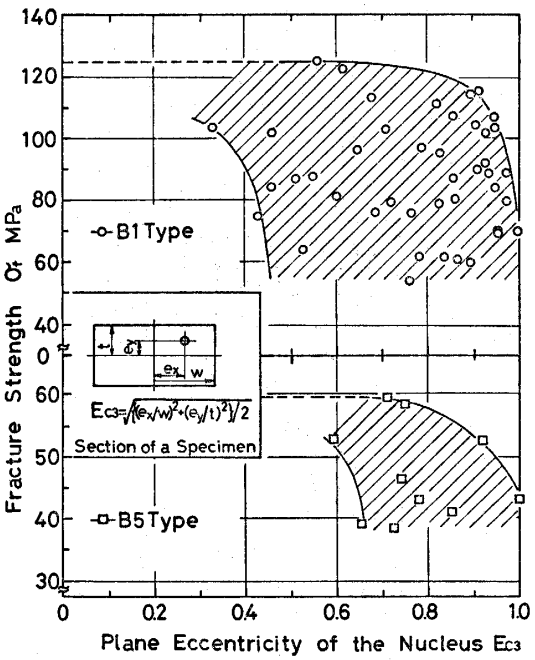

Fig. 5 Variation of fracture strength is shown with respect to the eccentricity of the nucleus in a fractured surface for the nonhomogeneous specimens including multiple micro-bubbles (about 0~500 μm dia.).

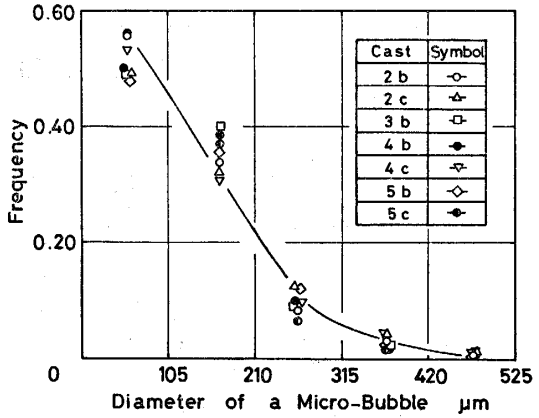

Fig. 6 Variation in frequency of finding a micro-bubble of the specified dia. in the nonhomogeneous specimens (B-Types).

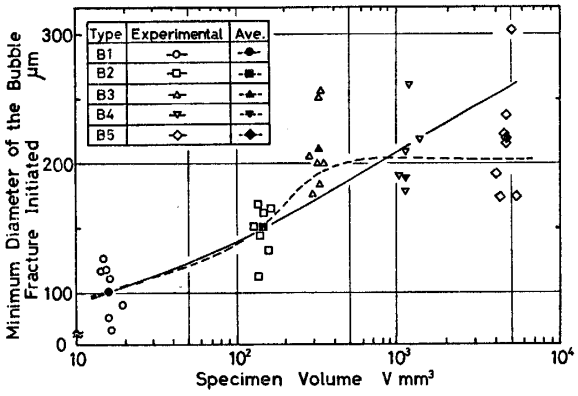

Fig. 7 Relationship between the minimum dia. of the bubble at which fracture initiated and its specimen volume.

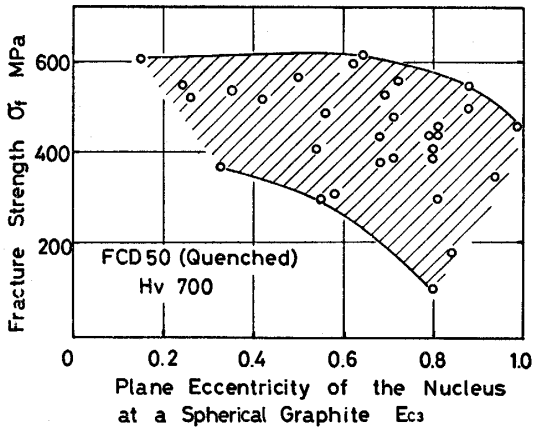

Fig. 8 Variation of fracture strength with respect to the eccentricity of the nucleus at a spherical graphite in FCD-50 in a fractured surface.

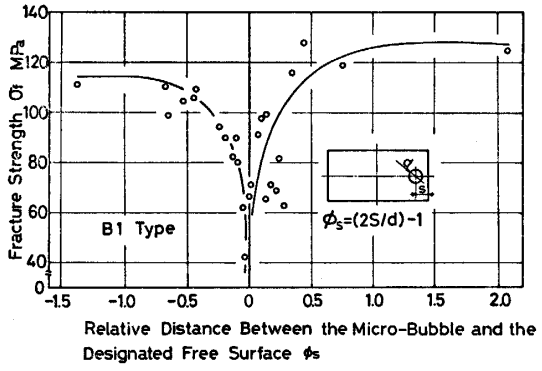

Fig. 9 Variation of fracture strength is expressed in the relative geometrical distance between the micro-bubble and the designated free surface in U. P..

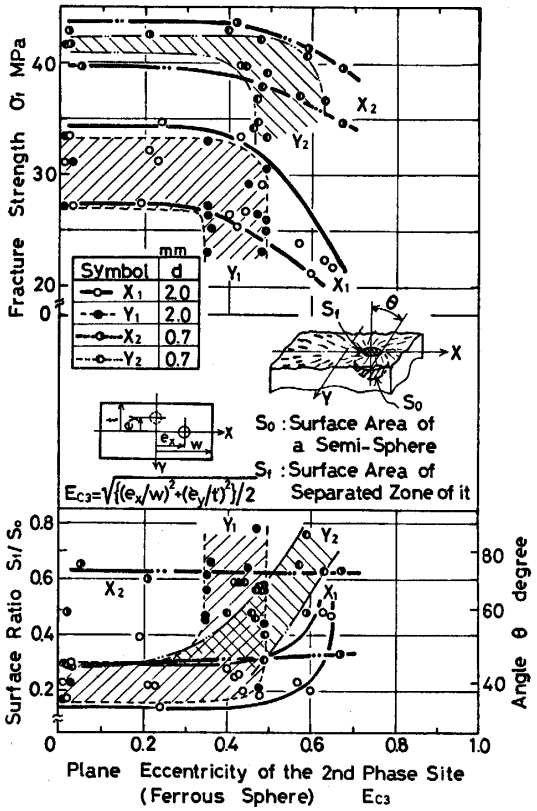

Fig. 10 Variations of fracture strength and the surface ratio are plotted with respect to the plane eccentricity of the second phase in a fractured surface for ferrous spheres of 0.7 and 2.0mm dia.. The corresponding angle (θ) from the axis of loading is also shown.

loss in strength with E_{C3} is again clear though the number of data points are less. The size distributions of micro-bubbles in specimens, B2～B5 in seven different casts, are studied and expressed in Fig. 6. We can see that as the bubble diameter becomes smaller the frequency of their existence in plastics is higher in each cast and that nearly half of them are in the size of about 100μm which can just be found in the photography used. A relationship between the specimen volume and the diameter of the bubble at which fracture initiated is shown in Fig. 7. A real or dotted line may be drawn to follow the increment in the bubble diameter as the specimen volume increases. We can learn that as the specimen becomes larger the critical diameter of the bubble at which fracture initiates increases and viceversa.

Fig. 8 shows the results on FCD-50, a nodular cast iron. The upper and lower bounds again indicate the loss in strength due to the increment in the plane eccentricity of a nucleus. In this practical material nodular graphite particles are fine of about 70μm and multiple graphites are seen in a fractured surface. The nucleus has, however, rela-

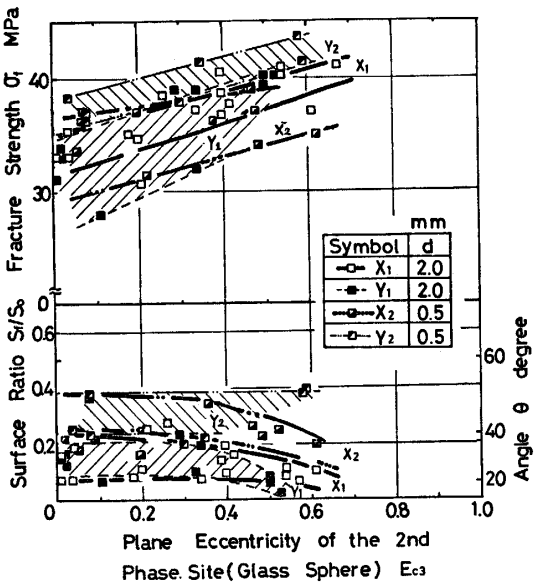

Fig. 11 Variations of fracture strength and the surface ratio are plotted with respect to the plane eccentricity of the second phase in a fracture surface for glass sphere of 0.5 and 2.0mm dia.. The corresponding angle (θ) from the axis of loading is also shown.

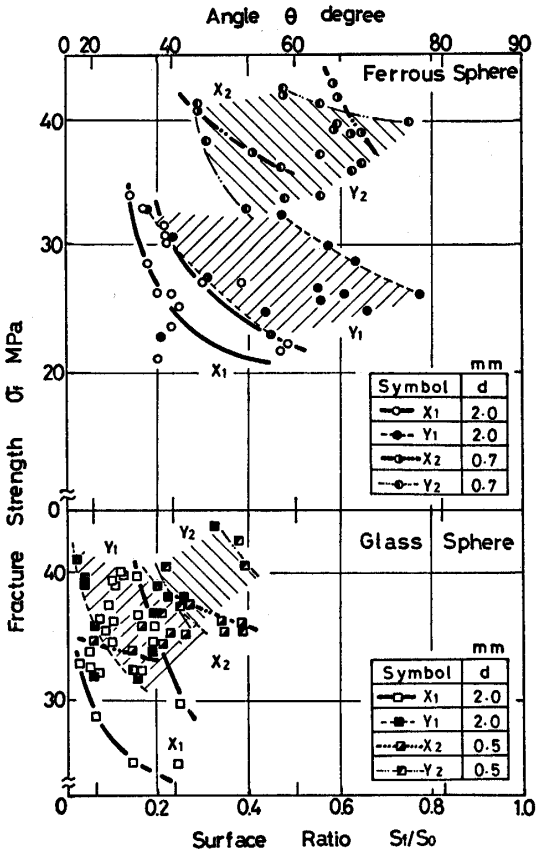

Fig. 12 Ralationships between fracture strength and the surface ratio are shown for the ferrous sphere in the top diagram and for the glass sphere in the bottom. The corresponding angle (θ) is also indicated.

tively clearly been observed.

We have so far analyzed the results with respect to the eccentricity which is referred to the center of the cross section of a specimen. On the other hand, the nucleus approaches closer to the free boundary as the eccentricity increases and the interaction between these two will be significant. To evaluate this, we define a relative distance, $\phi_s=(2s/d)-1$, where s is the minimum distance from the center of a sphere (a second phase or a nucleus) to the designated free boundary and d is the diameter of a sphere. Fracture strength decreases as the absolute value of the relative distance, ϕ_s, decreases as shown in Fig. 9 for B1 specimens and it approaches the minimum value at about $\phi_s=0$.

Next the results on specimens C1 and C2 are shown. Since these contain spheres artificially introduced in either the X or Y direction, the plane eccentricity, E_{C3}, given by only E_{C1} or E_{C2} can be calculated. The loss in strength for a ferrous sphere with the increment in the eccentricity in the X or Y direction is given in Fig. 10. The larger sphere of 2mm dia. indicates a stronger dependence of the eccentricity on the strength than the smaller one in the X direction. In the Y direction, that is the thickness direction, the larger one again shows a stronger dependence of it than the smaller one. These are also clearly shown in the relationship between the surface ratio (S_f/S_0) and the plane eccentricity in

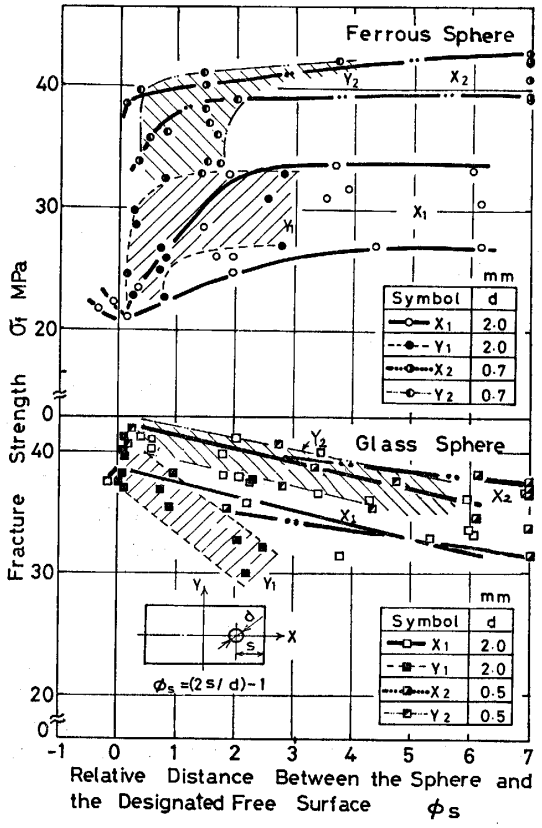

Fig. 13 Relationships between fracture strength and the relative geometrical distance between the sphere and the designated free surface are shown for the ferrous spheres in the top diagram and for the glass sphere in the bottom.

the bottom diagram, where the ratio indicates the degree of a separated zone surface of a sphere in fracture and is possibly related to interfacial bonding strength between a sphere and the plastic matrix. The top and bottom diagrams in Fig. 10 suggest that fracture strength increases as the surface ratio decreases except the case of X_2.

Results on the specimens having a glass sphere are given in Fig. 11. Fracture strength, both the upper and lower bounds in all four cases, increases as the plane eccentricity increases in contrast to the previous case. This may be due to the good bonding between a glass sphere and the glassy brittle plastic matrix. The surface ratio, in the bottom diagram, shows a decrease except the case of Y_2 as the plane eccentricity increases and this is again opposite to the previous example. The top and bottom diagrams in Fig. 11 suggest that fracture strength increases as the surface ratio decreases except the case mentioned.

Fig. 12 shows relationships between fracture strength and the surface ratio. In results on specimens containing a ferrous sphere (the top diagram), the upper and lower bounds, widely scatterd since all fractured with the different plane eccentricities, indicate the loss in strength due to the increment in the surface ratio. Results in the case of a glass sphere (the bottom), again show a similar relation as the above. The surface ratio in a ferrous sphere is extended to about 0.8 in contrast to 0.4 for the case of a glass sphere

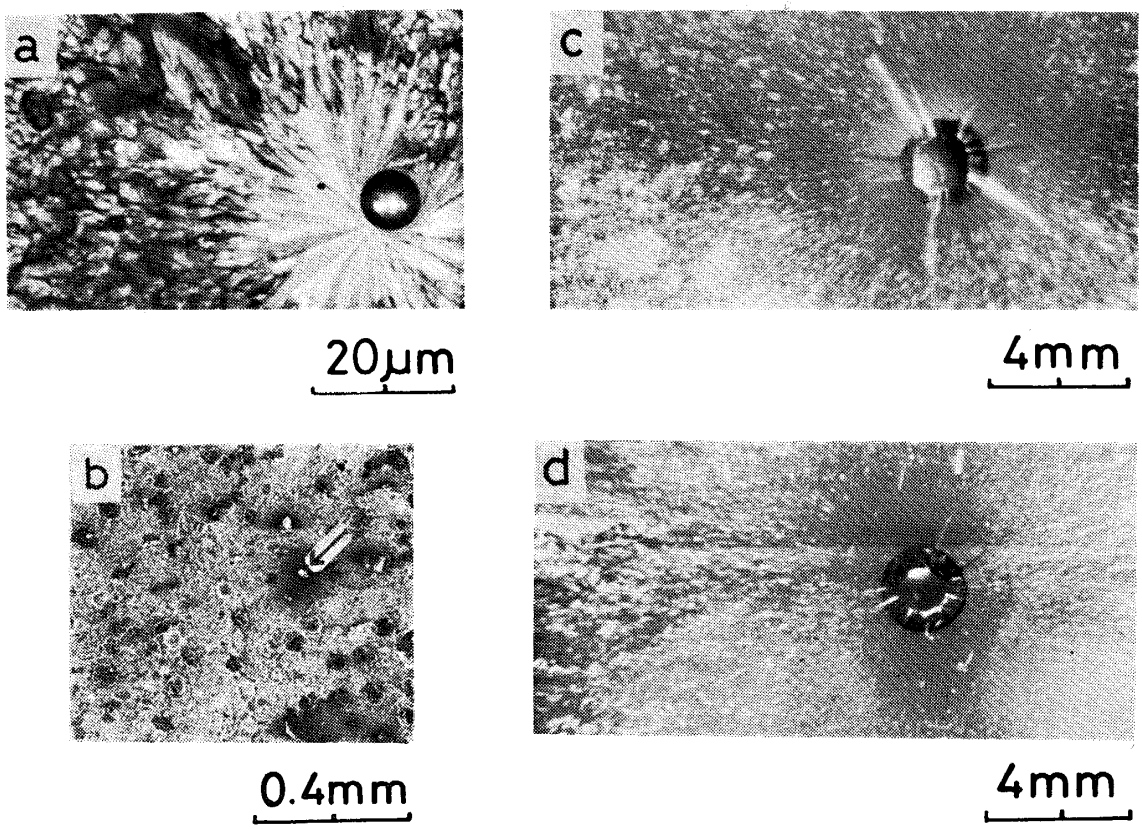

Photo 2 Fractured surfaces containing a bubble (a), nodular graphite particles (b) and a sphere located purposely (c, d). (c) shows a specimen having a ferrous sphere with the surface ratio (S_f/S_0) of 0.223 at the plane eccentricity (E_{c3}) of 0.329 and (d) a glass sphere with S_f/S_0 of 0.146 at E_{c3} of 0.20.

and this fact may prove that the latter has a good interfacial bonding.

Effect of a relative distance, ϕ_s, between a sphere and the free boundary on fracture strength is shown in Fig. 13. Fracture strength decreases as ϕ_s approaches to zero in specimens containing a ferrous sphere as expected. Variation in the Y direction is stronger than that in the X direction. On the other hand, fracture strength increases as ϕ_s approaches to zero in specimens containing a glass sphere and this may partly be due to the particle strengthening because of its good bonding between them. Photo 2 (a, b, c and d) shows fractured surfaces of specimens containing micro-bubbles, multiple nodular graphites, a ferrous and a glass spheres, respectively. In Photo (c and d) fracture initiated around the top of a sphere and their larger and smaller surface ratios are seen directly in photographs.

4. Discussion

We have reported the loss in fracture strength due to the eccentricity and the relative distance of a nucleation point in a fractured surface. These relations hold in the homogeneous, the nonhomogeneous and FCD-50 materials. Discussion is made on the following viewpoints.

4.1. The stress concentration at an eccentric site

The stress concentration factor of a hole at off site from the center of a specimen or around free boundary has been obtained experimentally by the photoelastic method[2]. The two dimensional results by Nishida[2] can be approximated to the following relationship in the limited extents of e/W and r/W by using the micro-computer.

$$K_t=[A\cdot exp\{B\cdot(r/W)\}\{C\cdot(r/W)+D-(e/W)^G\}]^{-1} \quad Where \quad G=E\cdot(r/W)^F$$

$$\begin{aligned} A &= 3.025\times10^{-1} & B &= 2.655 \\ C &= -1.560 & D &= 1.057 \\ E &= 7.729\times10^{-1} & F &= -9.612\times10^{-1} \end{aligned} \qquad \cdots(2)$$

The maximum stress fracture criterion gives the fracture strength ratio,

$$\sigma_f/\sigma_0=1/K_t=A\cdot exp\{B\cdot(r/W)\}\{C\cdot(r/W)+D-(e/W)^G\} \qquad \cdots(3)$$

This equation, though in the two dimensional relation, gives the relationship shown in Fig. 14 and the trend of losing strength with the increment of the eccentricity is very similar to the ones reported in the previous section. Since the nonhomogeneous plastics and FCD-50 cast iron have included various values of r/W and e/W, the summation of all these curves may give a wide band limited with the upper and lower bounds as in the experimental results. This may only be applicable to the nonhomogeneous materials having spherical cavities. The results in a ferrous sphere also shows a similar tendency of the loss in strength. However, the discrepancy in this case may stem from the difference in the location occuring the maximum stress. A spherical cavity in a continuum has the maximum stress at the equator ($\theta=\pi/2$) but a sphere dose at less angle ($\theta<\pi/2$).

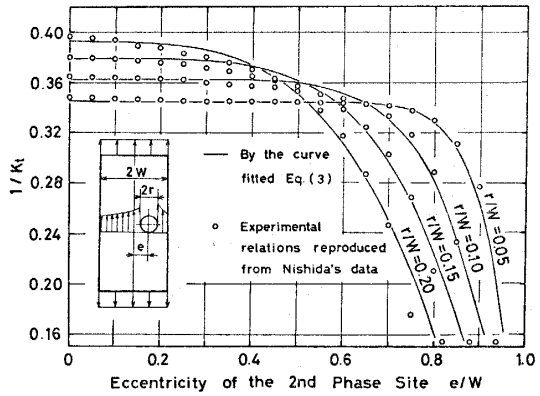

Fig. 14 Fracture strength ratio is expressed as a function of the eccentricity (e/w) of the maximum stress concentration site in the fractured surface.

4.2. A relative distance to the free boundary

The stress concentration factor of a spherical cavity around the free boundary has experimentally been given by the photoelastic method[2]. We interpolate the value for the material of having Poisson's ratio of 0.43 which we have employed here by using Nishida's results of 0.25 and 0.45. The inverse of the stress concentration factor is again plotted as a function of a relative distance, ϕ_s, of a cavity in Fig. 15, where $\phi_s = (2s/d)-1$, and s is the distance from the center of a sphere to the free boundary and d is the diameter of a sphere. The fracture strength ratio, that is $1/K_t$, decreases as the absolute value of ϕ_s decreases. This shows very similar relations given in Fig. 9 for the results of specimens having micro-bubbles and also in Fig. 13 for the case of containing a ferrous sphere (the top diagram) though the latter includes the effect of the interfacial bonding which varies the magnitude of the stress concentration.

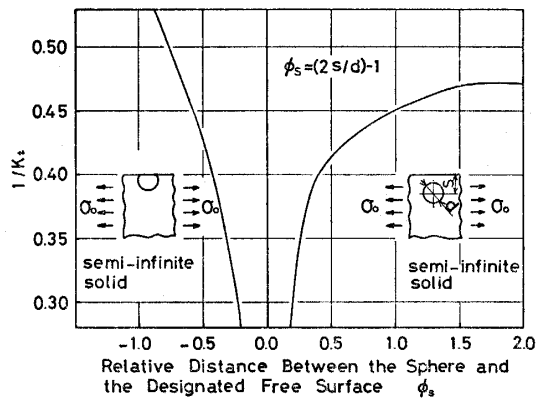

Fig. 15 A relationship between the reciprocal of the stress concentration factor and the relative geometrical distance between the sphere and the designated free surface in the elastic solid.

4.3. Interfacial bonding condition

The specimens containing a sphere always experience an interfacial bonding problem. Spheres employed here were examined their sphericities carefully and their surfaces were fully cleaned before use. A glass sphere showed a stronger interfacial bonding strength than a ferrous one in the preliminary test though the quantitative bonding strength in each case was not known because of its difficulties in experiments. Fig. 12 shows the dependence of fracture strength on the surface ratio which is strongly related to the interfacial bonding strength. Interfacial bonding will be broken at the top and bottom zones of a sphere under the applied load and the interfacial bonding will be strengthened by an addition of the radial stress component around the equatorial zone. In between two zones, the another zone of having different stress state may be formed, thus three differnt zones will be formed as the uniaxial load increases. This is shown schematically in Fig. 16. We define these three as the cap zone, the band zone I and the band zone II in a semi-sphere whose extents may be defined by the angles θ_1, θ_2 and θ_3, respectively. Wilson[4] has theoretically shown the stress distributions around a sphere in the non-Hertzian contact problem which contains a partial separation. Referring to his results three stresses may be qualitatively expressed as tabulated in Fig. 16, where P and N indicate tensile and compressive stresses, though the exact values are depend on the stress system applied and elastic constants of a sphere and the matrix. The experimental angle θ at which the exposed surface of a sphere appears, caluculated from the surface ratio, falls in the range of about 10~50 degree for a glass sphere and does in the range of 30~80 degree for a ferrous sphere. Comparing with the numerical results by Wilson, we suppose that fracturing at smaller angle ($\theta<28°$) may be hard to occur since σ_θ and $\sigma\psi$ are compressive and that fracturing due to σ_θ and $\sigma\psi$ at larger angle ($\theta>57°$) is easy to happen because both of possitive two increase by approaching the maximum at about $\theta=70°$. This, in a good agreement with the two dimensional results on the interfacial bonding[5),6)], can conclude that σ_θ plays an important role in the case of a ferrous sphere,

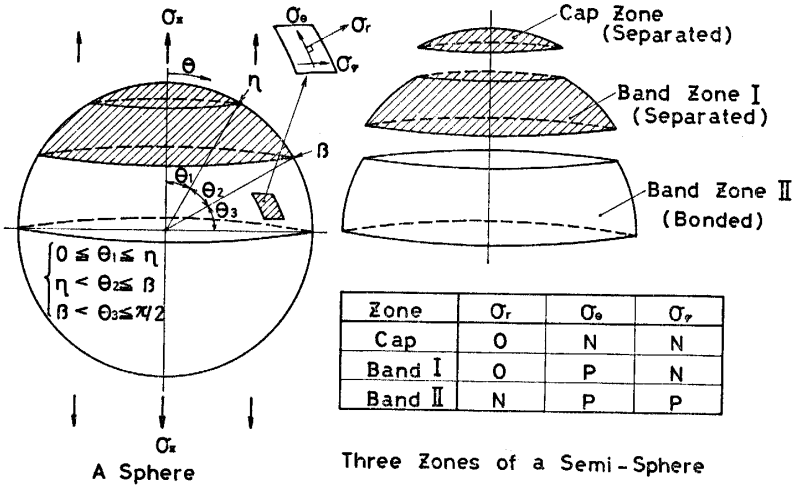

Zone	σ_r	σ_θ	σ_τ
Cap	0	N	N
Band I	0	P	N
Band II	N	P	P

Fig. 16 Three different bonding zones assumed between a second phase and a matrix and the kinds of stresses act.

where the interfacial bonding is relatively weak. In the case of a glass sphere a cap zone may work as a crack since fracture at lower angle ($\theta<28°$) has been often observed. If fracture strength is controlled predominantly by σ_θ, the application of the maximum stress criterion to this can well explain the strength dependence on the surface ratio. Stronger interfacial bonding, having a lower surface ratio with a smaller value of θ, should have higher fracture strength since the smaller value of σ_θ at the lower angle should be increased to the critical value of the material by increasing the applied stress. The reverse relation should hold too.

5. Summary

In studying brittle fracture strength of the homogeneous and the nonhomogeneous plastics, FCD-50 cast iron and the plastics containing a sphere, the following items are concluded on the size of a spherical second phase, the eccentricity of a nucleus (E_{C3}), the relative distance to the free boundary (ϕ_s) and the interfacial bonding.

1. The lower bound of fracture strength decreases as the eccectricity (E_{C3}) of a nucleus increases in the homogeneous plastics.

2. Fracture strength of the nonhomogeneous plastics containing micro-bubbles or a ferrous sphere and FCD-50 decreases with the increment of an eccentricity (E_{C3}) and with the decrement of a relative distance ($|\phi_s|$).

3. The diameter of a micro-bubble at which fracture nucleates increases with the increment in the specimen volume of the nonhomogeneous plastics.

4. Fracture strength of the nonhomogenous plastics containing a glass sphere indicates just the opposite trend to that of a ferrous sphere.

5. The tendency of losing fracture strength due to the eccentric nucleation can well be explained by the stress concentration at the off site.

6. The stronger interfacial bonding condition results in the smaller surface ratio (S_f/S_0) and higher fracture strength.

References

1) Tsuchida, E., Bulletin of the Japan Soc. of Mech. Eng., **41** [352], 3366-3378 (1955) (in Japanese)
2) Nishida, M., "Ouryoku Shuuchuu" (Morikita, Tokyo), p272-275, p523-529 (1967) (in Japanese)
3) Takimoto, A., Kawamoto, T., Kouhashi, Y. and Uchida, N., Proc. Symposium Japan Soc. Mech. Eng., Lecture Meeting No. 805-2, 41-43 (1980) (in Japanese)
4) Wilson, JR, H. B., "Axisymmetric Contact Stresses About a Smooth Elastic Sphere in an Infinite Solid Stressed Uniformly at Infinity" J. Appl. Mech., **34** [4], 960-966 (1967)
5) Stippes, M., Wilson, JR, H. B., and Krull, F.N., "A Contact Stress problem for a Smooth Disk in an Infinite Plate" Proc. 4th. U. S. Nat. Cong. Appl. Mech., **2**, 799-806 (1962)
6) Takimoto, A., Kawamoto, T., Kuniki, N. and Fujisawa, T., Proc. Symposium Japan Soc. Mech. Eng., lecture Meeting No. 815-1, 37-39 (1981) (in Japanese)